

A new probe of neutron skin thickness^{*}

SUN Xiao-Yan(孙小艳)^{1,2} FANG De-Qing(方德清)^{1;1)} MA Yu-Gang(马余刚)^{1;2)}
 CAI Xiang-Zhou(蔡翔舟)¹ CHEN Jin-Gen(陈金根)¹ GUO Wei(郭威)¹
 TIAN Wen-Dong(田文栋)¹ WANG Hong-Wei(王宏伟)¹
 ZHANG Guo-Qiang(张国强)^{1,2} ZHOU Pei(周培)^{1,2}

¹ Shanghai Institute of Applied Physics, Chinese Academy of Sciences, Shanghai 201800, China

² Graduate University of Chinese Academy of Sciences, Beijing 100049, China

Abstract: The correlation between neutron-to-proton yield ratio (R_{np}) and neutron skin thickness (δ_{np}) in neutron-rich projectile induced reactions is investigated within the framework of the Isospin-Dependent Quantum Molecular Dynamics (IQMD) model. The density distribution of the Droplet model is embedded in the initialization of the neutron and proton densities in the present IQMD model. By adjusting the diffuseness parameter of neutron density in the Droplet model for the projectile, the relationship between the neutron skin thickness and the corresponding R_{np} is obtained. The results show strong linear correlation between R_{np} and δ_{np} for neutron-rich Ca and Ni isotopes. It is suggested that R_{np} may be used as an experimental observable to extract δ_{np} for neutron-rich nuclei, which is very interesting in the study of the nuclear structure of exotic nuclei, the equation of state (EOS) of asymmetric nuclear matter and neutron-rich matter in astrophysics, etc.

Key words: IQMD, neutron-to-proton yield ratio, neutron skin thickness

PACS: 21.60.Cs, 25.70.Mn, 27.20.+n **DOI:** 10.1088/1674-1137/35/6/009

1 Introduction

The nuclear radius is one of the basic quantities of a nucleus. The proton root-mean-square (RMS) radius can be determined to very high accuracy via the charge radius measured by electromagnetic interactions, typically with an error of 0.02 fm or better for many nuclei [1]. In contrast, it is much more difficult to accurately determine the neutron density distribution of a nucleus experimentally [2]. Thus, the accuracy of the experimental neutron radius is much lower than that of the proton radius. However, the information of neutron density is of great importance to the study of nuclear structure for neutron-rich nuclei, atomic parity non-conservation, iso-vector interactions, and neutron-rich matter in astrophysics, etc. It is remarkable that the result of a single measurement has so many applications in the research fields of atomic, nuclear and astrophysics [3, 4].

A nucleus with a neutron number (N) larger than the proton number (Z) is expected to have a neutron skin (defined as the difference between the neutron and proton RMS radii: $\delta_{np} \equiv \langle r_n^2 \rangle^{1/2} - \langle r_p^2 \rangle^{1/2}$). The neutron skin thickness δ_{np} depends on the balance between various aspects of the nuclear force. The actual proton and neutron density distributions are determined by the balance between the isospin asymmetry and Coulomb force. δ_{np} is found to be related with a constraint on the equation of state (EOS) of asymmetric nuclear matter. Strong linear correlation between δ_{np} and L (the slope of symmetry energy coefficient C_{sym}), the ratio L/J (J is the symmetry energy coefficient at the saturation density ρ_0), $J - a_{sym}$ (a_{sym} is the symmetry energy coefficient of finite nuclei) are demonstrated [5]. This constraint is important for extrapolation of the EOS to high density and is hence useful for studying the properties of neutron stars [5–12]. Neutron skin thickness can carry a lot

Received 10 September 2010

^{*} Supported by National Natural Science Foundation of China (10775168, 10775167, 10979074, 10747163, 11035009), Major State Basic Research Development Program in China (2007CB815004) and Shanghai Development Foundation for Science and Technology (09JC1416800)

1) E-mail: dqfang@sinap.ac.cn

2) E-mail: ygma@sinap.ac.cn

©2011 Chinese Physical Society and the Institute of High Energy Physics of the Chinese Academy of Sciences and the Institute of Modern Physics of the Chinese Academy of Sciences and IOP Publishing Ltd

of information about the derivation of volume and surface symmetry energy, as well as nuclear incompressibility with respect to density. δ_{np} is significant in the study of the EOS in different theoretical models, such as Skyrme Hartree-Fock (SHF) [3, 4, 7–9, 11, 12], relativistic mean-field (RMF) [9, 10, 13], BUU model [14–16] and Droplet model [17]. Furthermore, neutron skin thickness can help to identify a nucleus with exotic structure. Thus the precise determination of δ_{np} for a nucleus becomes an important research subject in nuclear physics.

Several attempts have been made or suggested to determine the neutron density distribution, such as using proton scattering, interaction cross sections in heavy ion collisions at relativistic energies [18], parity violating measurements [3, 4, 7–9], and neutron abrasion cross sections in heavy ion collisions [19]. On the other hand, the neutron and proton transverse emission and double neutron-proton ratios have been studied as a sensitive observable of the asymmetry term of the nuclear EOS in the experiment [20] and different kinds of theoretical simulations [21–25].

In this paper, the relationship between δ_{np} and the ratio of the emitted neutron and proton yields ($R_{np} = Y_n/Y_p$) in neutron-rich projectile induced reactions is presented within the framework of the Isospin-Dependent Quantum Molecular Dynamics (IQMD) model. The possibility of extracting δ_{np} from R_{np} is investigated.

2 IQMD model

The QMD model is a many-body theory that can describe heavy ion collisions from intermediate energy to 2 GeV/nucleon [26]. It includes several important factors: initialization of the projectile and the target, nucleon propagation in the effective potential, NN collisions in a nuclear medium, and the Pauli blocking effect. A general review of the QMD model can be found in Ref. [27].

The IQMD model is based on the QMD model, which considers the effects of mean field, two-body NN collisions and Pauli blocking [26, 27]. Therefore, for an isospin-dependent reaction dynamics model, it is important to include isospin degrees of freedom with the above three components. In addition, the sampling of phase space of neutrons and protons in the initialization should be treated separately because of the large difference between neutron and proton density distributions for nuclei far from the β -stability line.

In the IQMD model, each nucleon is represented

by a Gaussian wave packet with a width \sqrt{L} (here $L=2.16 \text{ fm}^2$) centered on the mean position $\vec{r}_i(t)$ and the mean momentum $\vec{p}_i(t)$,

$$\psi_i(\vec{r}, t) = \frac{1}{(2\pi L)^{\frac{3}{4}}} \exp\left[-\frac{(\vec{r}-\vec{r}_i(t))^2}{4L}\right] \exp\left[\frac{i\vec{r}\cdot\vec{p}_i(t)}{\hbar}\right]. \quad (1)$$

The nuclear mean field in the IQMD model is determined as follows,

$$U(\rho, \tau_z) = \alpha \left(\frac{\rho}{\rho_0}\right) + \beta \left(\frac{\rho}{\rho_0}\right)^\gamma + \frac{1}{2}(1-\tau_z)V_c + C_{\text{sym}} \frac{\rho_n - \rho_p}{\rho} \tau_z + U^{\text{Yuk}}, \quad (2)$$

with $\rho_0=0.16 \text{ fm}^{-3}$ (the normal nuclear matter density). ρ , ρ_n and ρ_p are the total, neutron and proton densities, respectively. τ_z is the z th component of the isospin degree of freedom, which equals 1 or -1 for neutrons or protons, respectively. The coefficients α , β and γ are the parameters for the nuclear equation of state (EOS). C_{sym} is the symmetry energy strength due to the difference of neutron and proton. In the present work, we take $\alpha = -356 \text{ MeV}$, $\beta=303 \text{ MeV}$ and $\gamma=7/6$, which corresponds to the so-called soft EOS with an incompressibility of $K=200 \text{ MeV}$ and $C_{\text{sym}}=32 \text{ MeV}$ [11]. V_c is the Coulomb potential and U^{Yuk} is the Yukawa (surface) potential.

In the phase space initialization of the projectile and target, the density distributions of proton and neutron are distinguished from each other. The neutron and proton density distributions for the initial projectile and target nuclei in the present IQMD model are taken from the Droplet model [17, 28]. Using the density distributions of the Droplet model, we can get the initial coordinate of nucleons in nuclei in terms of the Monte Carlo sampling method. The momentum distribution of nucleons is generated by means of the local Fermi gas approximation,

$$P_{\text{F}}^i(\vec{r}) = \hbar[3\pi^2\rho_i(\vec{r})]^{1/3}, (i = n, p). \quad (3)$$

In the IQMD model, the nucleon's radial density can be written as

$$\rho(r) = \sum \frac{1}{(2\pi L)^{3/2}} \exp\left(-\frac{r^2+r_i^2}{2L} - \frac{L}{2rr_i}\right) \left[\exp\left(\frac{rr_i}{L}\right) - \exp\left(-\frac{rr_i}{L}\right) \right]. \quad (4)$$

In the Droplet model, we can change the diffuse-

ness parameter to get a different density,

$$\rho_i(r) = \frac{\rho_i^0}{1 + \exp\left(\frac{r - C_i}{f_i t_i / 4.4}\right)}, \quad i = n, p, \quad (5)$$

where ρ_i^0 is the normalization constant, which ensures that the integration of the density distribution equals the number of neutrons ($i=n$) or protons ($i=p$); t_i is the diffuseness parameter; C_i is the half density radius of neutron or proton determined by the Droplet model [17],

$$C_i = R_i[1 - (b_i/R_i)^2], \quad i = n, p, \quad (6)$$

where $b_i = 0.413f_i t_i$, and R_i is the equivalent sharp surface radius of neutron and proton. R_i and t_i are given by the Droplet model. A factor f_i is introduced by us to adjust the diffuseness parameter. In Ref. [29], Trzcińska et al. found that the half density radii for neutrons and protons in heavy nuclei are almost the same, but the diffuseness parameter for the neutron is larger than that for the proton. So we introduce the factor f_i to adjust the diffuseness parameter for the neutron. In the calculation for a neutron-rich nucleus, $f_p = 1.0$ is used in Eq. (5) for the proton density distribution, as in the Droplet model, while f_n in Eq. (5) is changed from 1.0 to 1.6. Different values of δ_{np} will be deduced from Eq. (5). We got the proton and neutron density distribution for ^{50}Ca in the situation of $f_n = f_p = 1.0$, as shown in Fig. 1. We also draw the neutron density that $f_n = 1.0 - 1.6$ together, as shown in Fig. 2.

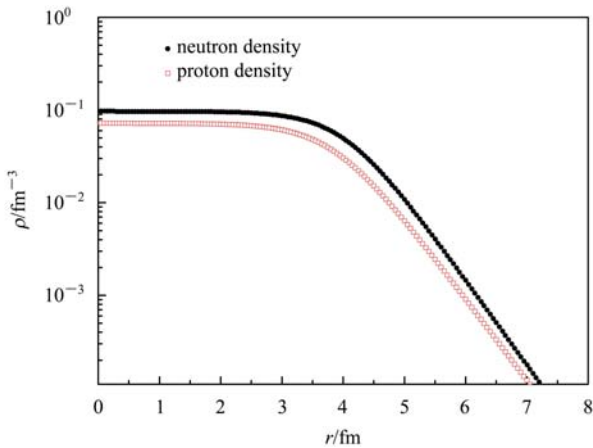


Fig. 1. The proton and neutron density distribution where $f_n = f_p = 1.0$ for ^{50}Ca calculated by the Droplet model.

To avoid taking an unstable initialization of projectile and target in the IQMD calculation, we only select the initialization samples of those nuclei that meet the required stability conditions for the bind-

ing energies and root mean square (rms) radii. Using the selected initialization phase space of nuclei in IQMD to simulate the collisions, the nuclear fragments are constructed by a coalescence model, in which nucleons with relative momentum smaller than $P_0 = 300 \text{ MeV}/c$ and relative distance smaller than $R_0 = 3.5 \text{ fm}$ will be combined into a cluster.

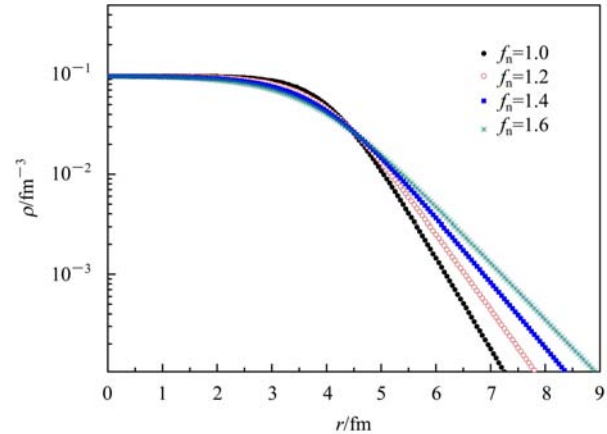


Fig. 2. The neutron density distribution where $f_n = 1.0, 1.2, 1.4, 1.6$ for ^{50}Ca calculated by the Droplet model.

3 Calculation and discussion

The collision processes of some Ca and Ni isotopes with ^{12}C target at 50 A MeV are simulated using the IQMD model. The fragments including neutrons and protons formed during the evolution of the collision are constructed by the coalescence method. The yield ratio R_{np} of the emitted neutrons and protons can be calculated from the yields of the produced neutrons and protons. By changing the factor f_n in the neutron density distribution of the Droplet model for the projectile, different values of δ_{np} and the corresponding R_{np} are obtained. Thus we can obtain the correlation between R_{np} and δ_{np} . In the calculation, the time evolution of the dynamical process was simulated until $t = 200 \text{ fm}/c$. The calculated R_{np} is stable after 150 fm/c, as shown in Fig. 3, so we accumulate the emitted neutrons and protons between 150 fm/c and 200 fm/c in order to improve the statistics. The R_{np} from different ranges of the reduced impact parameter for $^{54}\text{Ca} + ^{12}\text{C}$ are plotted in Fig. 4. The reduced impact parameter is defined as b/b_{max} with b_{max} being the maximum impact parameter. From Fig. 4, we can see that R_{np} rises as δ_{np} increases. With δ_{np} being fixed, R_{np} also becomes larger with increasing reduced impact parameter. This means that R_{np} from peripheral collisions is usually larger than

that from central collisions. Strong linear correlation between R_{np} and δ_{np} of the projectile, especially for $0.8 < b/b_{\max} < 1.0$, is exhibited in Fig. 4. This indicates that R_{np} is very sensitive to δ_{np} of the projectile, especially in peripheral collisions. The main purpose of the present study is to investigate the relationship between R_{np} and the neutron skin thickness of the projectile. The R_{np} from different ranges of the kinetic energy for emitted neutrons and protons for $^{54}\text{Ca}+^{12}\text{C}$ are plotted in Fig. 5. From the results shown in Fig. 5, we can see that R_{np} with the kinetic energy greater than 40 MeV are larger than those with other kinetic energy ranges. The lower kinetic energy range includes a relatively large portion of neutrons or protons emitted from the target. On the other hand, the larger kinetic energy range

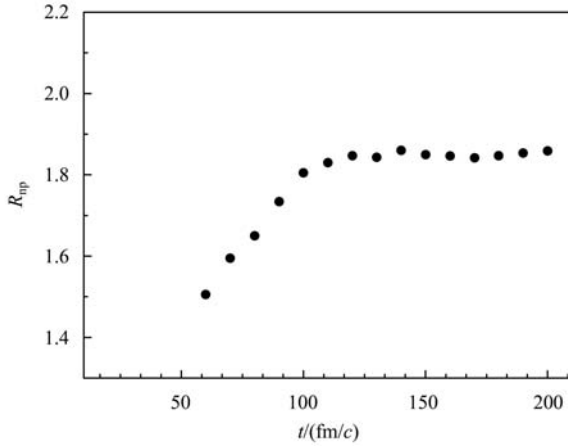


Fig. 3. The evolution time dependence of R_{np} for $^{54}\text{Ca}+^{12}\text{C}$ at 50 A MeV.

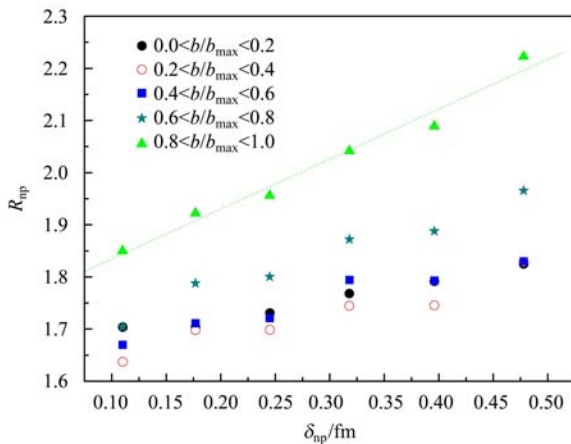


Fig. 4. The dependence of R_{np} on the neutron skin thickness of the projectile for $^{54}\text{Ca}+^{12}\text{C}$ at 50 A MeV under the condition of kinetic energy of nucleons (E_k) > 40 MeV. Different symbols are used for different ranges of the reduced impact parameter, as shown in the legend. The dotted lines just guide the eye.

includes many neutrons and protons ejected from mid-rapidity, which is the overlap zone between the projectile and the target [30]. In this context, the nucleons with moderate kinetic energy are more suitable for the study of R_{np} versus δ_{np} . Since the projectile is a neutron-rich nucleus, stronger correlation between R_{np} and δ_{np} is expected for nucleons that have moderate kinetic energy coming from the projectile rather than for those that have larger kinetic energy from mid-rapidity or for those that have smaller kinetic energy from the target.

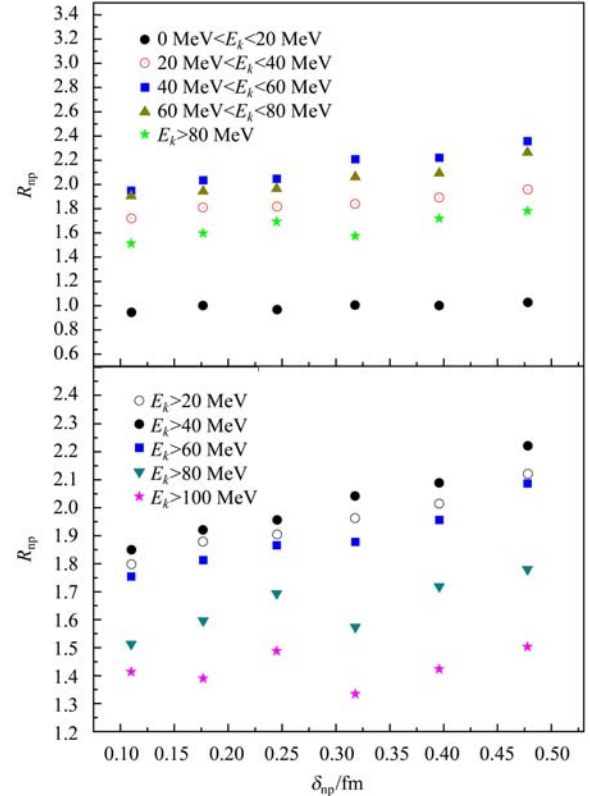


Fig. 5. The dependence of R_{np} on the neutron skin thickness under the condition of reduced impact parameter from 0.8 to 1.0 for $^{54}\text{Ca}+^{12}\text{C}$ at 50 A MeV. Different symbols are used for different ranges of the kinetic energy ranges, as shown in the legend. The dotted lines just guide the eye.

For a systematic study, reactions of other Ca and Ni isotopes, such as $^{52,54,56}\text{Ca}$ and $^{60,62,64,66,70}\text{Ni}$, are also calculated. The results with the reduced impact parameter from 0.8 to 1.0 and the kinetic energy greater than 40 MeV are shown in Fig. 6 and Fig. 7, respectively. A strong linear relationship between R_{np} and δ_{np} is also observed for all projectiles. From Fig. 6 and Fig. 7, a linear function ($R_{np} = a + b \cdot \delta_{np}$) can describe the correlation between R_{np} and δ_{np} well for

both Ca and Ni isotopes. The dependence between R_{np} and δ_{np} is fitted using this linear function. The mean slopes for Ca and Ni isotopes are 0.83 and 0.67, respectively.

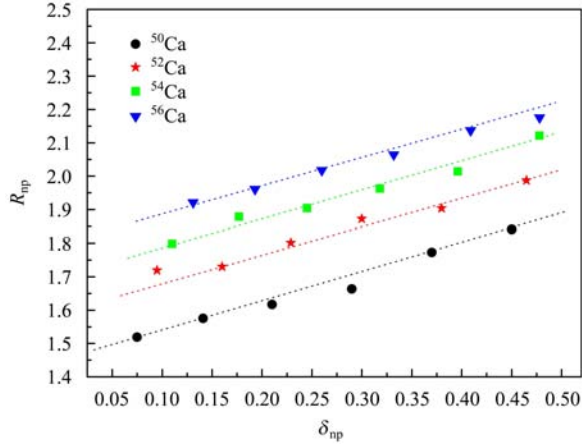


Fig. 6. The dependence of R_{np} on neutron skin thickness under the condition of kinetic energy greater than 40 MeV and $0.8 < b/b_{max} < 1.0$ for $^{50,52,54,56}\text{Ca} + ^{12}\text{C}$ at 50 A MeV. Different symbols are used for different Ca isotopes, as shown in the legend. The dotted lines just guide the eye. For detail, see the text.

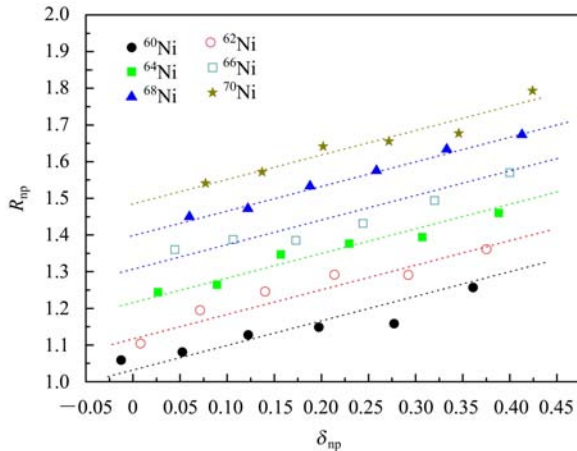


Fig. 7. The dependence of R_{np} on neutron skin thickness under the condition of kinetic energy greater than 40 MeV and $0.8 < b/b_{max} < 1.0$ for $^{60,62,64,66,70}\text{Ni} + ^{12}\text{C}$ at 50 A MeV. Different symbols are used for different Ni isotopes, as shown in the legend. The dotted lines just guide the eye. For detail, see the text.

From the above discussions, R_{np} could be viewed as a sensitive observable of δ_{np} for the projectile. If the produced neutrons and protons are measured by experiment, it is possible to extract δ_{np} from the neutron-to-proton yield ratio R_{np} . From the fitted

slope values, the estimated error of δ_{np} is around 0.1 fm if the uncertainty of R_{np} is less than 5%. It should be pointed out that this uncertainty does not take into account the error arising from the determination of the impact parameter, which is always an important issue in the studies of nuclear reactions in the energy range of our calculation. To achieve high resolution, well defined experimental determination of the centrality of the reaction is required for this method.

The neutron excess ($I = (N-Z)/A$) dependence of neutron skin thickness for four parameter sets (NL3, NL-SH, SkM*, SIII) in the Droplet model and self-consistent extended Thomas-Fermi (ETF) calculations have been investigated by Warda et al. [31].

Differences in the neutron skin thickness among different predictions increase with the increase in I . To distinguish which potential parameter set or method is closer to the experimental data, a higher resolution measurement on the neutron skin thickness is required for stable nuclei having small I in comparison with the nuclei far from the stability line having a large I value. From their results, the neutron skin thickness by different calculations varies from 0.01 fm to 0.11 fm at $I = 0.11$. In this sense, it will be capable of distinguishing different theoretical predictions when $I > 0.11$ by extracting δ_{np} from R_{np} measurement, which the present paper proposes. In other words, the present method will be more feasible for heavy nuclei or intermediate mass nuclei far from the β -stability line.

4 Conclusions

In summary, we have carried out calculations on the relationship between R_{np} and the neutron skin thickness. The simulated data for Ca and Ni isotope induced reactions show a good linear correlation between R_{np} and δ_{np} for neutron-rich projectile. It is suggested that R_{np} is used as an experimental observable to extract the neutron skin thickness for a neutron-rich nucleus. When the neutron skin thickness of one isotope is obtained, we can get some information about the EOS in different theoretical models such as Skyrme Hartree-Fock, relativistic mean-field and the BUU model. From the isotope dependence of the neutron skin thickness, a lot of information about the derivation of volume and surface symmetry energy, as well as nuclear incompressibility with respect to density, could be extracted. This is very important for the study of the EOS of asymmetric nuclear matter.

References

- 1 Fricke G, Bernhardt C, Heilig K, Schaller L A, Schellenberg L, Shera E B, Dejager C W. *Data Nucl. Data Tables*, 1995, **60**: 177
- 2 Ray L, Hoffmann G W, Coker W R. *Phys. Rep.*, 1992, **212**: 223
- 3 Horowitz C J, Pollock S J, Souder P A, Michaels R. *Phys. Rev. C*, 2001, **63**: 025501
- 4 Danielewicz P. *Nucl. Phys. A*, 2005, **727**: 233
- 5 Centelles M, Roca-Maza X, Viñas X, Warda M. *Phys. Rev. Lett.*, 2009, **102**: 122502
- 6 Klimkiewicz A, Paar N, Adrich P, Fallot M, Boretzky K, Aumann T, Cortina-Gil D, DattaPramanik U, Elze Th W, Emling H, Geissel H, Hellström M, Jones K L, Kratz J V, Kulesa R, Nociforo C, Palit R, Simon H, Surówka G, Sümmerer K, Vretenar D, Waluś W. *Phys. Rev. C*, 2007, **76**: 051603(R)
- 7 CHEN L W, KO C M, LI B A. *Phys. Rev. C*, 2005, **72**: 064309
- 8 Brown B A. *Phys. Rev. Lett.*, 2000, **85**: 5296
- 9 Yoshida S, Sagawa H. *Phys. Rev. C*, 2004, **69**: 024318
- 10 Suzuki T, Geissel H, Bochkarev O, Chulkov L, Golovkov M, Fukunishi N, Hirata D, Irnich H, Janas Z, Keller H, Kobayashi T, Kraus G, Münzenberg G, Neumaier S, Nickel F, Ozawa A, Piechaczek A, Roeckl E, Schwab W, Sümmerer K, Yoshida K, Tanihata I. *Nucl. Phys. A*, 1998, **630**: 661
- 11 Sammarruca F, LIU P. *Phys. Rev. C*, 2009, **79**: 057301
- 12 LIU M, WANG N, LI Z X, WU X Z. *Chin. Phys. Lett.*, 2006, **23**: 804
- 13 Bhagwat A, Gambhir Y K. *Phys. Rev. C*, 2006, **73**: 054601
- 14 MA Y G, SHEN W Q, FENG J, MA Y Q. *Phys. Lett. B*, 1993, **302**: 386
- 15 MA Y G, SHEN W Q, FENG J, MA Y Q. *Phys. Rev. C*, 1993, **48**: 850
- 16 CAI X Z, SHEN W Q, FENG J, FANG D Q, MA Y G, SU Q M, ZHANG H Y, HU P Y. *Chin. Phys. Lett.*, 2000, **17**: 565
- 17 Myers W D, Swiatecki W J. *Ann. Phys. A*, 1974, **84**: 186; Myers W D, Swiatecki W J. *Nucl. Phys. A*, 1979, **336**: 267
- 18 Suzuki T, Geissel H, Bochkarev O, Chulkov L, Golovkov M, Hirata D, Irnich H, Janas Z, Keller H, Kobayashi T, Kraus G, Münzenberg G, Neumaier S, Nickel F, Ozawa A, Piechaczek A, Roeckl E, Schwab W, Sümmerer K, Yoshida K, Tanihata I. *Phys. Rev. Lett.*, 1995, **75**: 3241
- 19 MA C W, FU Y, FANG D Q, MA Y G, CAI X Z, GUO W, TIAN W D, WANG H W. *Chin. Phys.*, 2008, **17**: 1216
- 20 Famiano M A, LIU T, Lynch W G, Mocko M, Rogers A M, TSANG M B, Wallace M S, Charity R J, Komarov S, Sarantites S G, Sobotka L G, Verde G. *Phys. Rev. Lett.*, 2006, **97**: 052701
- 21 MA Y G, SU Q M, SHEN W Q, HAN D D, WANG J S, CAI X Z, FANG D Q, ZHANG H Y. *Phys. Rev. C*, 1999, **60**: 024607
- 22 ZHANG Y X, Danielewicz P, Famiano M, LI Z X, Lynch W G, TSANG M B. *Phys. Lett. B*, 2008, **664**: 145
- 23 TSANG M B, ZHANG Y X, Danielewicz P, Famiano M, LI Z X, Lynch W G, Steiner A W. *Phys. Rev. Lett.*, 2009, **102**: 122701
- 24 LI B A, CHEN L W, YONG G C, ZUO W. *Phys. Lett. B*, 2006, **634**: 378
- 25 Rizzo J, Colonna M, Di Toro M. *Phys. Rev. C*, 2005, **72**: 064609
- 26 Aichelin J, Rosenhauer A, Peilert G, Stoecker H, Greiner W. *Phys. Rev. Lett.*, 1987, **58**: 1926
- 27 Aichelin J. *Phys. Rep.*, 1991, **202**: 233
- 28 Myers W D, Schmidt K H. *Nucl. Phys. A*, 1983, **410**: 61
- 29 Trzcińska A, Jastrzebski J, Lubiniński P, Hartmann F J, Schmidt R, Edigy T V, Klos B. *Phys. Rev. Lett.*, 2001, **87**: 082501
- 30 MA Y G, Natowitz J B, Wada R, Hagel K, WANG J, Keutgen T, Majka Z, Murray M, QIN L, Smith P, Alfaro R, Cibor J, Cinausero M, Masri Y El, Fabris D, Fioretto E, Keksis A, Lunardon M, Makeev A, Marie N, Martin E, Martinez-Davalos A, Menchaca-Rocha A, Nebbia G, Prete G, Rizzi V, Ruangma A, Shetty D V, Souliotis G, Staszal P, Veselsky M, Viesti G, Winchester E M, Yennello S J. *Phys. Rev. C*, 2005, **71**: 054606
- 31 Warda M, Viñas X, Roca-Maza X, Centelles M. *Phys. Rev. C*, 2009, **80**: 024316